Henriksson, M., Flärdh, O., Mårtensson, J. (2017)
Optimal Speed Trajectories Under Variations in the Driving Corridor.
In: *IFAC-PapersOnLine* (pp. 12551-12556). Elsevier
https://doi.org/10.1016/j.ifacol.2017.08.2194

Optimal Speed Trajectories Under Variations in the Driving Corridor

Manne Henriksson [*,**] **Oscar Flärdh** [**] **Jonas Mårtensson** [*]

[*] *Department of Automatic Control and the Integrated Transport Research Lab, KTH Royal Institute of Technology, 100 44 Stockholm, Sweden*
[**] *Scania CV AB, 151 87 Södertälje, Sweden*
e-mail: manneh@kth.se, oscar.flardh@scania.com, jonas1@kth.se

Abstract: The optimal speed trajectory for a heavy-duty truck is calculated using the Pontryagin's maximum principle. The truck motion depends on controllable tractive and braking forces and external forces such as air and rolling resistance and road slope. The velocity of the vehicle is restricted to be within a driving corridor which consists of an upper and a lower boundary. Simulations are performed on data from a test cycle commonly used for testing distribution driving. The data include road slope and a speed reference, from which the driving corridor is created automatically. The simulations include a sensitivity analysis on how changes in the parameters for the driving corridor influence the energy consumption and trip time. For the widest driving corridor tested, 15.8 % energy was saved compared to the most narrow corridor without increasing the trip time. Most energy was saved by reducing the losses due to braking and small amounts of energy were saved by reducing the losses due to air resistance. Finally, optimal trajectories with the same trip time derived from different settings on the driving corridor are compared in order to analyse energy efficient driving patterns.

Keywords: Nonlinear and optimal automotive control, Trajectory and Path Planning, Intelligent driver aids.

1. INTRODUCTION

A major concern for the industry of heavy-duty vehicles is how to reduce the fuel consumption. The reason for this is a combination of legal, environmental and economic factors. Since about one third of the total cost for a typical European long haulage company consists of fuel (Scania CV AB, 2014), a lot of money can be saved by gaining knowledge on how to reduce the consumption. The problem of reducing the fuel consumption for a given driving mission can be posed as an optimal control problem, in which an optimal speed trajectory is the result, see Sciarretta et al. (2015) for an overview of such methods in automotive applications. A common way for calculating the optimal speed trajectory is to use Pontryagin's maximum principle. This has succesfully been done with applications to rail bounded trains in Khmelnitsky (2000) and Golovitcher and Iakov (2001) and to an electric car in Petit and Sciarretta (2011). The optimization using this method involves integration of an adjoint-state variable which is a continuous function in the absence of constraints on the speed. In the precence of such constraints however, the adjoint-state variable may have different types of discontinuities. A theoretical description of such discontinuities is given in Hartl et al. (2015) and practical examples in train applications are given in Wong (2008).

Funding provided by Swedish Governmental Agency for Innovation Systems (VINNOVA) through the FFI program is gratefully acknowledged.

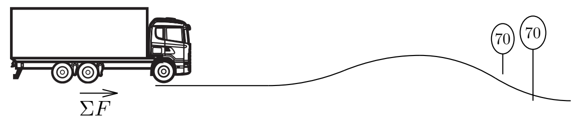

Fig. 1. A truck is driving in an environment containing road elevation and varying speed restrictions while being influenced by the resulting force ΣF.

Another method for solving optimal control problems is to use a Model Predictive Controller (MPC), which has received great attention recently. The MPC can often solve the optimization problem online using some prediction horizon. In Kamal et al. (2013) this is done while taking a preceding vehicle into account, in Henzler et al. (2015) the focus is on reducing calculation time and in Kirches et al. (2013), the gear selection is also taken into account.

In order to set the boundary conditions for the allowed speed during optimization problems involving an optimal speed trajectory, a natural way is to study statistics extracted from real vehicle operation. In Themann and Eckstein (2012), a total of 49 subjects were studied when approaching a traffic light under naturalistic circumstances. From the resulting decelerations, the mean value and standard deviation are calculated and used in order to adapt the driving strategy to driver preferences. In Themann et al. (2015), these statistics are used in order to create a driving corridor which consists of the maximum and minimum allowed velocities.

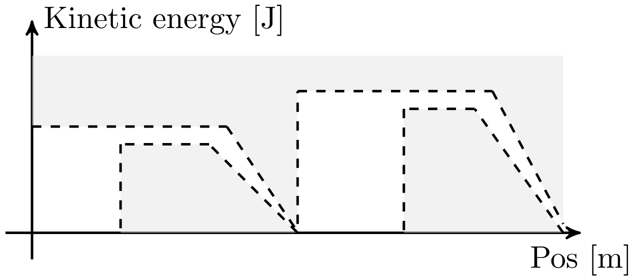

Fig. 2. The kinetic energy of the vehicle must be within the area between the dashed lines, referred to as the driving corridor.

This paper investigates further the optimal control problem formulated in Henriksson et al. (2016), where the energy consumption and trip time is minimized for a heavy-duty truck. This is illustrated in Fig. 1, where a truck subject to resistive natural forces from air and rolling resistance drives in an environment including varying altitude and speed restrictions. This paper focuses on how the solution to the optimal control problem depends on the boundary conditions. The most important boundary conditions are the upper and lower limits for the allowed kinetic energy. These limits form the driving corridor, which is conceptualized in Fig. 2. Given the driving corridor, different values on the weighting between the cost of consumed energy and trip time give different optimal trajectories.

There are two main contributions of this paper. The first is a sensitivity analysis on the influence of variations on the boundary conditions of the optimization problem developed in Henriksson et al. (2016) with respect to energy consumption and trip time. Solutions originating from different driving corridors but with the same resulting trip time are compared thoroughly. A detailed analysis of the contributions from different types of losses as well as an analysis of the characteristics of the resulting speed trajectories is performed on these solutions. The second contribution is the development of an algorithm to automatically create a driving corridor from a speed reference and statistics from real truck operation. This paper uses statistics from live heavy-duty truck operation and not from experiments as in Themann and Eckstein (2012) and Themann et al. (2015). In addition, all types of decelerations are considered, i.e., from any start speed to any end speed.

2. PROBLEM FORMULATION

This section is mainly a summary of Henriksson et al. (2016) and describes the vehicle model, the optimization problem and the optimal solution.

2.1 Vehicle model

A simplified model of a heavy-duty truck is used with the kinetic energy $K(s)$, s being the position, as the state variable. The position is used as the independent variable rather than time, because the driving corridor and altitude data are given as functions of position. The derivative of the kinetic energy with respect to position is given by

Table 1. Natural constants and vehicle parameters.

Parameter	Value
mass (m)	26 000 kg
maximum power (P_{max})	250 kW
drag coefficient (C_d)	0.5
air density (ρ)	1.292 kg·m^{-3}
vehicle cross-sectional area (A)	10 m^2
rolling resistance coefficient (c_{r0})	0.006

$$\frac{dK(s)}{ds} = F_t(s) + F_b(s) + F_w(K(s)) + F_g(s) \tag{1}$$

where $F_t(s)$ is the controllable tractive force, $F_b(s)$ is the controllable braking force, $F_w(K(s))$ is the sum of the resistive environmental forces and $F_g(s)$ is the gravitational force. The resistive environmental forces are given by

$$F_w(K(s)) = F_a(K(s)) + F_r(s) \tag{2}$$

where the contribution from the air resistance $F_a(K(s))$ is given by

$$F_a(K(s)) = -\rho A C_d \frac{K(s)}{m} \tag{3}$$

and the contribution from rolling resistance is given by

$$F_r(s) = -mgc_{r0}\cos(\alpha(s)) \tag{4}$$

where ρ is the air density, A is the vehicle frontal area, C_d is the air drag coeffient, m is the vehicle mass, c_{r0} is the coefficient for the rolling resistance, g is the gravitational constant and α is the road slope. The gravitational force $F_g(s)$ is given by

$$F_g(s) = -mg\sin(\alpha(s)). \tag{5}$$

The parameters used for calculating the values of the environmental forces are set by following Wong (2008) and can be seen together with the vehicle parameters in Table 1. The tractive and braking forces are restricted by velocity dependent limits

$$0 \leq F_t(s) \leq F_{t_{max}}(K(s)), \tag{6a}$$

$$F_{b_{max}}(K(s)) \leq F_b(s) \leq 0. \tag{6b}$$

The vehicle is modelled to have constant maximum tractive and braking power, $P_{t_{max}}$ and $P_{b_{max}}$ respectively. The maximum tractive and braking forces $F_{t_{max}}$ and $F_{b_{max}}$ are then given by the relation $F = P\sqrt{\frac{m}{2K(s)}}$.

2.2 Optimization problem

The objective of the optimization problem is the minimization of the cost function

$$\min_{F_t, F_b} \int_0^S (F_t(s) + P_c\sqrt{\frac{m}{2K(s)}})ds \tag{7}$$

over the distance S. The variable P_c is a weighting factor between energy and time and can be thought of as a power constant in time consisting of e.g. energy to keep the engine running or cost for personnel per time unit. This can be seen by noting that $\int_0^S \sqrt{\frac{m}{2K(s)}}ds$ gives the trip time. The contribution from this cost will however not be included in the comparison between the energy consumption of simulations with different driving corridors, since such comparison would require the same value on P_c. The kinetic energy is bounded by an upper limit K_u and a lower limit K_l such that

$$K_l(s) \leq K(s) \leq K_u(s). \tag{8}$$

The driving corridor is defined as the area between the functions $K_l(s)$ and $K_u(s)$.

2.3 Optimal solution

As in Henriksson et al. (2016), Pontryagin's maximum principle is used in order to solve the optimization problem. From (1) and (7) the Hamiltonian

$$H = F_t[\psi - 1] + F_b[\psi] - P_c\sqrt{\frac{m}{2K(s)}} + \psi\left(F_w(K(s)) + F_g(s)\right) \quad (9)$$

is created. The variable ψ is the adjoint-state variable with differential equation

$$\frac{d\psi}{ds} = [1-\psi]\frac{\partial F_t}{\partial K} - \psi\frac{\partial F_b}{\partial K} - \frac{P_c}{(2K(s)/m)^{3/2}} - \psi\frac{dF_w}{dK} + \mu_u - \mu_l. \quad (10)$$

The variables μ_u and μ_l are non-negative Lagrange multipliers which can cause discontinuities in ψ when the kinetic energy becomes or stops being equal to the upper or lower limit. According to Pontryagin's maximum principle, the optimal solution must maximize the Hamiltonian. Pointwise maximization of (9) yields the following policy for the controllable forces F_t and F_b depending on the value of ψ:

Full power: If $\psi(s) > 1$ then $F_t(s) = F_{t_{max}}$ and $F_b(s) = 0$, called the full power regime, since maximum tractive force will maximize the Hamiltonian.

Partial power: If $\psi(s) = 1$ then $0 \leq F_t(s) \leq F_{t_{max}}$ and $F_b(s) = 0$, called the partial power regime. The optimal control is not given directly by the Hamiltonian here.

Coasting: If $0 < \psi(s) < 1$ then $F_t(s) = 0$ and $F_b(s) = 0$, called the coasting regime, since both the tractive and the braking force should be equal to zero in order to maximize the Hamiltonian.

Partial braking: If $\psi(s) = 0$ then $F_t(s) = 0$ and $F_{b_{max}} \leq F_b(s) \leq 0$, called the partial braking regime. The optimal control is not given directly by the Hamiltonian here.

Full braking: If $\psi(s) < 0$ then $F_t(s) = 0$ and $F_b(s) = F_{b_{max}}$, called the full braking regime, since maximum braking force will maximize the Hamiltonian.

As argued in Henriksson et al. (2016), partial power can occur at either the upper or lower speed limit. It can also occur at the so called stabilization value, which is given by the unique solution to

$$\frac{P_c}{(2K(s)/m)^{3/2}} + \frac{dF_w}{dK} = 0 \quad (11)$$

denoted K_s. Partial power can occur at this value only if $K_l(s) < K_s < K_u(s)$. Partial braking can only occur at the upper speed limit. Varying the value of P_c in the problem formulation will cause the solution to find different values for the kinetic energy during partial power, i.e. at the upper or lower speed limit or at the stabilization energy K_s.

3. THE DRIVING CORRIDOR

The driving corridor consists of varying upper and lower bounds on the allowed kinetic energy, $K_u(s)$ and $K_l(s)$ respectively. These will be centered around a given reference speed trajectory on sections where the reference is constant. However, on sections where the speed reference is lowered, the driving corridor is set based on historical data from decelerations in live operation. By creating the driving corridor in this way, the vehicle is restricted to decelerate in a way that similar vehicles normally do.

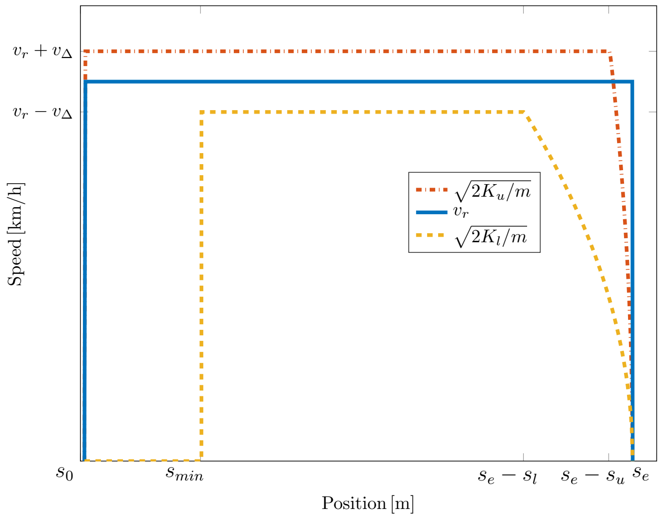

Fig. 3. Reference speed trajectory and driving corridor.

3.1 Analysing deceleration data

As explained in Henriksson et al. (2016), historical driving data collected from a heavy-duty truck used in distribution application were used in order to calculate the mean value and standard deviation for the decelerations. From this data, two look-up functions for extracting these data are created. The function

$$d_\mu = d_\mu(v(s_1), v(s_2)) \quad (12)$$

gives the mean deceleration from a start speed $v(s_1)$ to an end speed $v(s_2)$. The function

$$\Sigma = \Sigma(v(s_1), v(s_2)) \quad (13)$$

gives the standard deviation of the deceleration from a start speed $v(s_1)$ to an end speed $v(s_2)$. The data were collected during 39 000 km of driving and a total number of 20 160 decelerations were recorded.

3.2 Creating the driving corridor

The driving corridor is created from a total distance of 63 km of an internal test cycle used at Scania CV AB for distribution applications. The cycle data consist of an altitude profile and a desired reference speed trajectory $v_r(s)$. The reference speed trajectory is a piecewise constant function with a total number of 57 stops. The reference speed is constant between two positions where the reference speed is 0 km/h. When the value of the reference speed trajectory is being changed, for instance from a section with the constant value 90 km/h to 0 km/h, this is done from one sample to the next. When the driving corridor is constructed, statistics collected from real operation are used in order to set the driving corridor during decreasing speed limits. The creation of the driving corridor from a reference speed trajectory can be seen in

Fig. 3, where the solid line is the reference speed trajectory and the dashed lines form the driving corridor. Two inputs are required in order to create it. The first one is the allowed deviations from the reference speed trajectory v_Δ given in km/h. The second input is the number of standard deviations n_Σ that the vehicle should be allowed to deviate from the average deceleration when the reference speed is decreased. For each position where the reference speed is decreased, i.e., where $v_r(s_2) < v_r(s_1)$ for two positions $s_2 > s_1$, the required distance needed for the vehicle to decelerate from $v_r(s_1) \pm v_\Delta$ to $v_r(s_2) \pm v_\Delta$ is calculated as s_u and s_l respectively using constant deceleration. In the test cycle on which the simulations in this papers are performed, all decelerations are performed to a complete stop, i.e. $v_r(s_2) = 0$. For this special case, both the upper and lower limits of the driving corridor are set to 0 rather than $v_r(s_2) \pm v_\Delta$. In Fig. 3, the reference speed trajectory is lowered at position s_e and the positions $s_e - s_l$ and $s_e - s_u$ need to be calculated. The distance between the passed and upcoming upper limit s_u is calculated from the maximum allowed deceleration $d_\mu(v_r(s_1), v_r(s_2)) + n_\Sigma \Sigma(v_r(s_1), v_r(s_2))$ and the distance between the passed and upcoming lower limit s_l is calculated by using $d_\mu(v_r(s_1), v_r(s_2)) - n_\Sigma \Sigma(v_r(s_1), v_r(s_2))$. The variables v_Δ and n_Σ are chosen as part of the simulation and the variables $d_\mu(v_r(s_1), v_r(s_2))$ and $\Sigma(v_r(s_1), v_r(s_2))$ are functions of the start and end speed for the decelerations and are given by the data as discussed in section 3.1.

When the value of the speed reference is increased, i.e. when $v_r(s_2) > v_r(s_1)$ as is the case at position s_0 in Fig. 3, the driving corridor does not consider statistics from accelerations of the vehicle. Instead, a restriction that the truck must use full power until the new lower limit $v_r(s_2) - v_\Delta$ is reached is imposed. This distance is denoted s_{min}. Since a heavy-duty truck most often accelerates more slowly than other traffic, this is not a disturbing restriction from the perspective of other traffic participants. By letting the driving corridor start at the position where the vehicle reaches the lower limit $v_r(s_2) - v_\Delta$ by using full power, this way of accelerating is the only feasible one.

3.3 Reference following

Setting different values on P_c in (7) will influence the solution regarding which speed will be kept during partial power. For instance, a high value on P_c will put a high weight on minimizing trip time compared to minimizing energy consumption. The implication of this over the full driving mission will be that the vehicle will drive at the maximum allowed speed most the time. The same goes for the opposite: a low value of P_c will give a resulting trajectory where the vehicle drives at the minimum allowed speed most of the time. However, if the value of P_c is set to be equal to the kinetic energy at the reference value v_r, then partial power can occur at this value. The solution derived from such approach is still optimal on a subinterval where the reference speed is constant. Letting P_c vary on intervals with different reference speed will give a solution that is not necessarily optimal over the full driving mission. This is still a valuable approach, because it can be used as a benchmark for comparison. Using this approach while setting small values on v_Δ and n_Σ will create a trajectory that follows the reference speed where the reference speed is constant and follows the mean rate of deceleration where the reference speed is decreased. Since small deviations within the driving corridor is still allowed, coasting will still be used to a small extent in order to save energy. The reason for using such approach for benchmarking instead of creating a driving corridor with $v_\Delta = 0$ and $n_\Sigma = 0$ is that the latter approach would create an unrealistic driving behaviour. For instance, the vehicle would start braking at the same time as it stops using tractive force when entering a downhill.

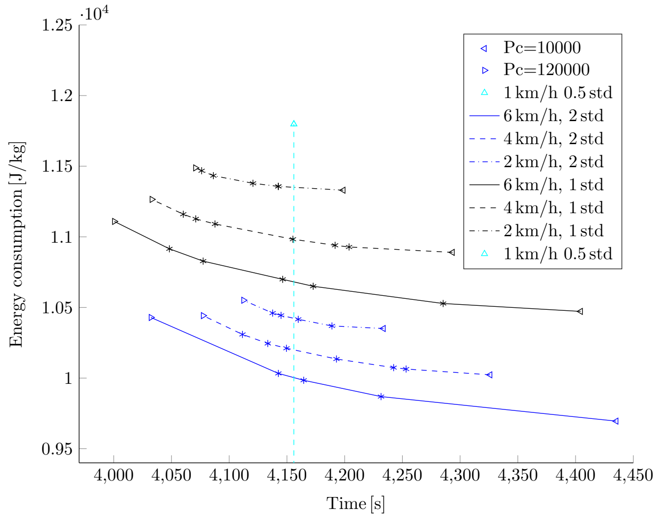

Fig. 4. Simulation results showing energy consumption and trip time.

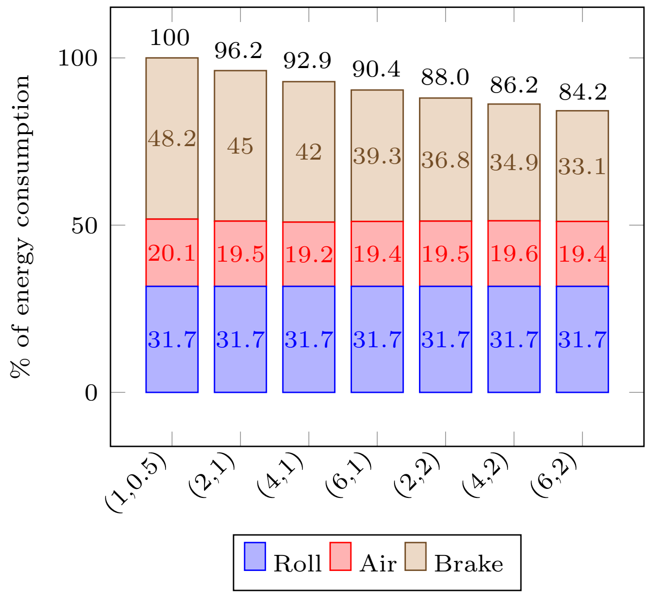

Fig. 5. Energy losses for each simulation parameters (v_Δ,n_Σ) as percentage of total losses for the benchmark value (1,0.5).

4. SIMULATION RESULT

Simulations were performed using Matlab on 63 km of a distribution test cycle described in section 3.2. In order to create the driving corridor, the procedure from section 3 was used. Energy consumption and trip time can be seen

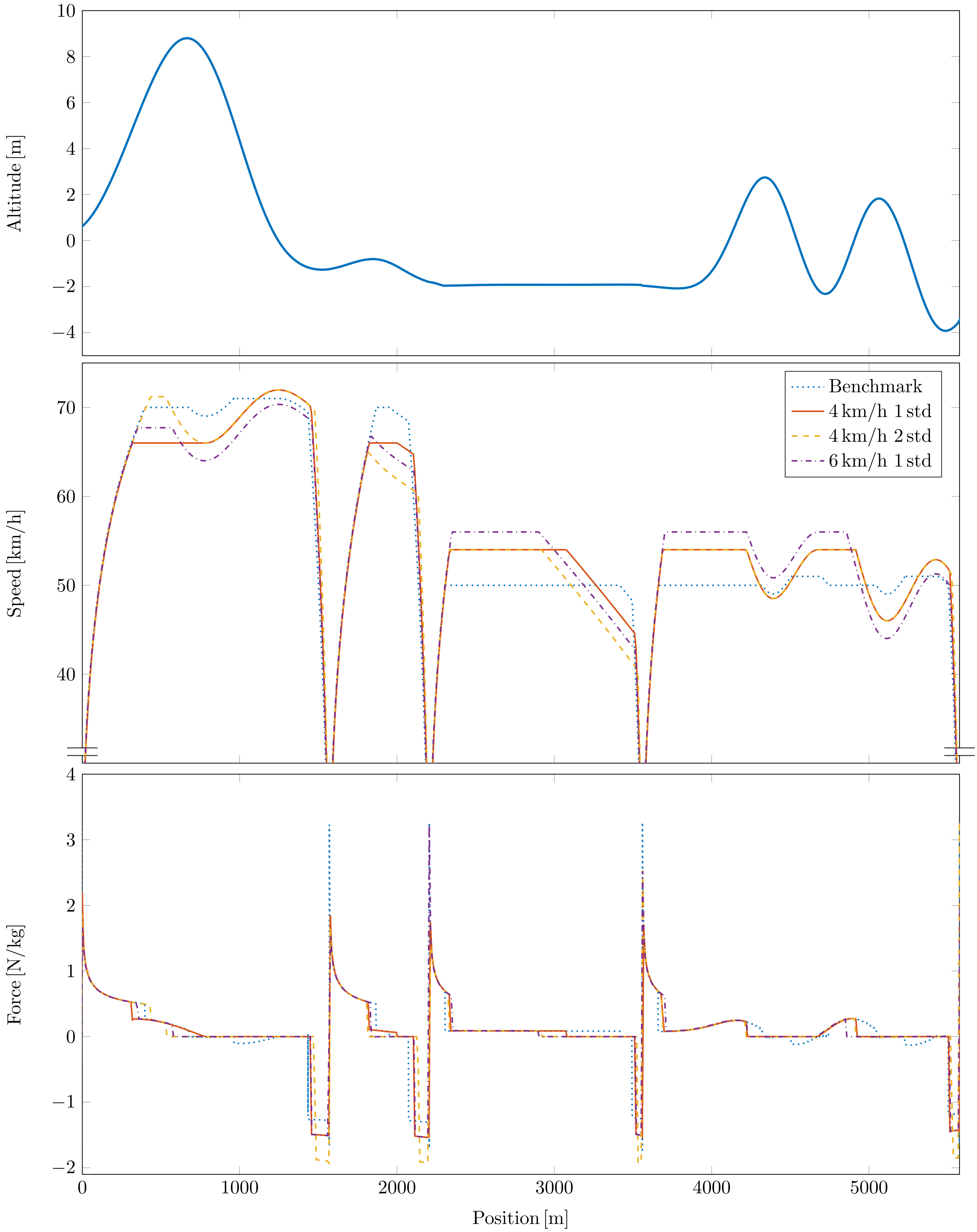

Fig. 6. Altitude, speed trajectories and input force from simulations using different settings on the driving corridor. The value of the weight P_c is adjusted such that each solution has approximately the same trip time.

in Fig. 4. Points on the same line all belong to simulations with the same driving corridor but with different values on the weighting factor P_c. It can be noted that the lines span different ranges of trip time which is because a wider driving corridor gives a wider range of possible trip times. It can be seen that all three solutions having $n_\Sigma = 2$ consume less energy than those using $n_\Sigma = 1$, even if these driving corridors are narrower in terms of v_Δ. The trip time of the simulation by setting P_c according to the reference speed trajectory as discussed in section 3.3 was 4160 s. It is in the following referred to as the benchmark solution. For the simulations using other settings for the driving corridor, the solution that best corresponds to the benchmark solution in terms of trip time is selected. None of these simulations has a trip time deviating more than 0.3 % from the benchmark solution.

Next, these solutions, all with approximately the same trip time but with different settings on the driving corridor, are compared in terms of categorized energy losses and resulting speed trajectories. The distribution of energy losses caused by air resistance (3), rolling resistance (4) and braking is shown in Fig. 5. It can be seen that the losses due to rolling resistance remain the same, the losses due to air resistance have only small deviations while the big difference between the simulation cases are the losses due to braking. A wider driving corridor allows for bigger deviations in the speed trajectory and thus the possibility to avoid braking to a greater extent. It can also be seen in Fig. 5 that the simulation from the driving corridor $(v_\Delta, n_\Sigma) = (2, 2)$ is more energy efficient than the simulation from the driving corridor with $(v_\Delta, n_\Sigma) = (6, 1)$. This indicates that increasing the allowed deviations during decelerations is more important than increasing the allowed deviations during constant speed.

A selected part showing four sections of the resulting speed trajectories can be seen in Fig. 6. Since all simulations have trip times that deviate at most 0.3 % from the benchmark solution, a trajectory that is slower than another on some section must compensate for this by driving faster on some other section. A general pattern is that solutions with a wider driving corridor save time by driving faster on sections where the speed reference is low and save energy by driving slower where the speed reference is high. This can be explained by the fact that the air resistance is proportional to the square of the velocity. In Fig. 6, it can be seen that the other solutions have a lower velocity than the benchmark solution on the first two sections where the reference speed trajectory is high, while they have higher velocities on the two last sections where the reference speed trajectory is low. A wider driving corridor also allows for using coasting to a greater extent. In Fig. 6, this can be seen clearly on the third section. The solutions with wider driving corridors start coasting already at around position 3000 m while the benchmark solution does not start coasting until at around position 3400 m.

5. CONCLUSION

The simulations described in this paper have shown that great amounts of energy can be saved without increasing the trip time by improving the control of the tractive and braking forces of the vehicle. This can be done by stating the driving mission as an optimal control problem and solving it using Pontryagin's maximum principle. By creating a driving corridor based on traffic data, the improvements can be done without the vehicle deviating from a normal traffic flow. By dividing the wasted energy into categories, it has been shown that the potential of saving energy when using a wider driving corridor primarily comes from the reduction of energy wasted on braking. For this specific test cycle, it has also been concluded that widening the driving corridor in terms of standard deviations during decelerations reduces the energy consumption more than widening it in terms of deviations from a constant speed reference.

REFERENCES

Golovitcher, I.M. and Iakov, M. (2001). Energy efficient control of rail vehicles. *Systems, Man, and Cybernetics, 2001 IEEE International Conference on*, 1, 658–663.

Hartl, R., Sethi, S., and Raymond, V. (2015). A Survey of the Maximum Principles for Optimal Control Problems with State Constraints. *SIAM Rev.*, Vol. 37(2), 274–297.

Henriksson, M., Flärdh, O., and Mårtensson, J. (2016). Optimal Speed Trajectory for a Heavy Duty Truck Under Varying Requirements. In *2016 IEEE 19th International Conference on Intelligent Transportation Systems*, 820–825.

Henzler, M., Buchholz, M., and Dietmeyer, K. (2015). Inhomogeneous Model Predictive Control Horizon Discretization for an Urban Truck Energy Efficient Driving Application. In *2015 IEEE 18th International Conference on Intelligent Transportation Systems*, 430–436.

Kamal, M.A.S., Mukai, M., Murata, J., and Kawabe, T. (2013). Model predictive control of vehicles on urban roads for improved fuel economy. *IEEE Transactions on Control Systems Technology*, 21(3), 831–841.

Khmelnitsky, E. (2000). On an optimal control problem of train operation. *IEEE Transactions on Automatic Control*, 45(7), 1257–1266.

Kirches, C., Bock, H.G., Schl, J.P., and Sager, S. (2013). Mixed-integer NMPC for predictive cruise control of heavy-duty trucks. In *European Control Conference 2013*, volume 4, 4118–4123.

Petit, N. and Sciarretta, A. (2011). Optimal drive of electric vehicles using an inversion-based trajectory generation approach. In *18:th IFAC World Congress*, 14519–14526.

Scania CV AB (2014). Annual Report 2014. URL `https://www.scania.com/group/en/scania-annual-report-2014-2/`.

Sciarretta, A., De Nunzio, G., and Ojeda, L.L. (2015). Optimal Ecodriving Control: Energy-Efficient Driving of Road Vehicles as an Optimal Control Problem. *IEEE Control Systems Magazine*, 35(5), 71–90.

Themann, P. and Eckstein, L. (2012). Modular Approach To Energy Efficient Driver Assistance Incorporating Driver Acceptance. In *IEEE Intelligent Vehicles Symposium*, 1023–1028.

Themann, P., Eckstein, L., and Bock, J. (2015). Optimisation of energy efficiency based on average driving behaviour and driver's preferences for automated driving. *IET Intelligent Transport Systems*, 9(1), 50–58.

Wong, J. (2008). *Theory of Ground Vehicles.* Wiley-Interscience. John Wiley & Sons, 4th edition.